IEEE Access
Multidisciplinary | Rapid Review | Open Access Journal

Received April 3, 2020, accepted April 14, 2020, date of publication April 20, 2020, date of current version May 7, 2020.

Digital Object Identifier 10.1109/ACCESS.2020.2988919

Empirical Model Including the Statistics of Location Variability for the Over-Rooftop Path in the 32 GHz Band

YOUNGKEUN YOON[1], SANGWOOK PARK[2], AND JONG HO KIM[1]

[1]Electronics and Telecommunications Research Institute, Daejeon 34129, South Korea
[2]Division of Electronic and Electrical Engineering, College of Information and Communication Engineering, Daegu University, Gyeongsan 38453, South Korea

Corresponding authors: YoungKeun Yoon (ykyoon@etri.re.kr) and SangWook Park (wave@daegu.ac.kr)

This work was supported by the Institute of Information & Communications Technology Planning & Evaluation (IITP) funded by the Government of South Korea (MSIT (RRA)) (Development of Radio Propagation Analysis Model Based on Clutter of Slop Path) under Grant 2019-0-00054.

ABSTRACT This paper proposes a propagation prediction model including the statistics of location variability for over-rooftop path in millimeter-wave suburban environments. The predictive model derived from the measurement was developed to analyze the propagation characteristic of the signal according to the distance within the area of a millimeter-wave band or future fifth-generation service band. The measurement was carried out using a radio wave characteristic measurement system called the channel sounder, and the signal transmitted to the air was captured to make the received signal level data. The measurement system was constructed to predict spatial propagation characteristics by transmitting and receiving a signal with a 500 MHz bandwidth, and this system was capable of predicting characteristics of a signal that varied with space and time by capturing wideband multipath signals. Measurements were performed in a small town covered with low-rise commercial restaurants or houses. The transmission signal propagated through the rooftops of low-rise houses on average 10 meters high. Their multipath signal arrived at a receiving station located under the roof of the house through reflection, diffraction, and scattering mechanisms. The change in the signals due to the variation in location was measured up to a distance of about 500 meters from the transmitter. The basic transmission loss prediction model with a probability density distribution was analyzed and interpreted based on these measurements. In practice, it was necessary to statistically model for path loss according to the characteristics of the location due to the various environment changes, such as buildings and roads. The proposed prediction model derived from the measurement data reflects the propagation impact on over-rooftop paths in a small town and includes the statistics of location variability in line-of-sight and non-line-of-sight regions.

INDEX TERMS Measurement, basic transmission loss, probability, location variability, rooftop.

I. INTRODUCTION

Feasibility studies on basic transmission loss characteristics based on separation distance of a transceiver from 20 GHz to 70 GHz frequency bands are routinely conducted [1]–[5]. In the case of millimeter-waves, the attenuation characteristics along the path are large, so a horn antenna with a higher directional gain than an omni-directional antenna was used for real environment measurements. Measurements were made after defining the environment for buildings and roads in the actual urban environment to characterize the signal transmitted through the over-rooftop path below the seventh floor of the city center or through the below-rooftop path of a low-rise building. In consideration of the mobile communication service in high-speed mobile vehicles, measurements using high-speed trains in suburban areas were also carried out. In the mobile communication environment, operators want to provide high-speed, high-capacity services over the air using a spectrum of at least 400 MHz to 1 GHz for the radio spectrum in the millimeter-wave band [6]. References [7]–[9] provide a basic transmission loss prediction model based on the distance to the over-rooftop path in a short-range outdoor environment, but not for the site-general basic transmission loss model for non-line-of-sight (NLoS) in suburban or urban low-rise environments.

The associate editor coordinating the review of this manuscript and approving it for publication was Giorgio Montisci.

In particular, as with the below-rooftop path, the location variation property [7] for line-of-sight (LoS) and NLoS is required but not currently provided for the over-rooftop path. For the above-rooftop path, the site-specific path loss model [7] assumes that the construction of the building with the same building height is infinitely long without a gap between buildings, unlike the actual environment. It is hard to find such a simple building configuration in a real environment. In a real environment, the rooftop of the actual building may be flat, but often it is sloped or the structure of the building is complex. In [10], a clutter-based site-specific propagation prediction model is provided to predict the performance of a low-altitude vehicle-to-ground communication system. As an application example, the propagation loss characteristics due to obstacles caused by building-based clutter are considered when low-altitude vehicles move and communicate with receivers on the ground. Radio waves propagated by low-altitude vehicles in the air reach the receivers on the ground through the over-rooftop path of the building clutter, and only the effects of diffraction characteristics are considered; the effects on multipath characteristics, such as overall building-based reflections, were not considered. Reference [11] explains the effect of propagation characteristics on free space loss due to the movement of surrounding objects or the position of the receiver in the open area of the millimeter-wave band (28 GHz, 38 GHz) for 5G service. In [12]–[15], the characteristics of path loss according to the distance of the multipath in the indoor commercial area or the urban outdoor environment are explained. Although the transmitter antenna position is relatively high above 10 meters, the antenna positions of the transmitter and receiver are still considered lower than the surrounding buildings. However, existing data and forecasting methods for the median path loss do not reflect realistic environments with partially open spaces between houses or other variations in suburban small towns.

In this paper, to provide a realistic assessment of millimeter-wave propagation in a suburban environment, we developed a prediction model for the over-rooftop path based on the statistical analysis scheme for location variation of below-rooftop prediction provided by the Recommendation ITU-R P.1411 [7]. To express the statistics of location variability in our empirical model, the best-fit distributions are extracted from the cumulative distribution function (CDF) based on the measurement data. Finally, we present the location percentage site-general modeling and the measurement data on 32 GHz bands together with the site-specific prediction model for propagation above rooftop provided by the Recommendation ITU-R P.1411 [7].

II. MEASUREMENT DESCRIPTION

A. MEASUREMENT SYSTEM

We developed a broadband 32 GHz measurement sounder capable of detecting multipath signals with time- and space-varying characteristics. For the configuration of the broadband measurement sounder, the 32 GHz millimeter wave radio frequency part (RF part) was combined with the existing intermediate-frequency part (IF part) and the baseband processing part (BB processing part) [12], [16]. The RF part with a bandwidth of 500 MHz operates at the center frequency of 32.4 GHz. The sounder, as the transmission to the reception system, was composed of independent transmitter and receiver modules that included a 32 GHz-RF part, 5.2 GHz-IF part, BB processing part, electric and mechanical control part, and so on. Figure 1 shows the block diagram of measurement system.

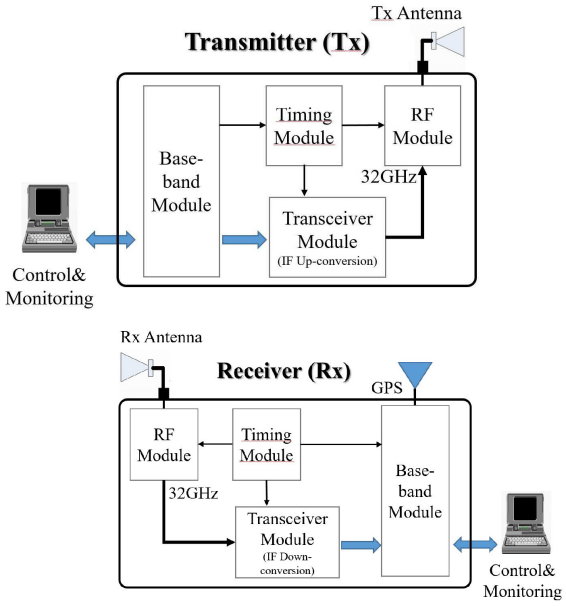

FIGURE 1. Block diagram of measurement system: Transmitter and Receiver.

TABLE 1. The main parameters of measurement system [17].

Operating center frequency	32.4 GHz
Channel band-width	500 MHz
Transmission conducting power	27 dBm/500 MHz
Transmission signal	4096 PN sequence
Tx antenna (beam-width, directional gain)	horn type (15°, 21 dBi)
Rx antenna (beam-width, directional gain)	horn type (15°, 21 dBi)
Tx antenna height on the ground level	44 m
Rx antenna height on the ground level	1.5 m
Number of Tx antenna	1
Number of Rx antenna	1

The broadband 32 GHz measurement sounder is described in Table 1. A transmitter (Tx) was mounted on the roof of the tall building. A receiver (Rx) was placed above the moving cart. Pseudo-random noise (PN) sequences at a length of 4096 were continually generated at the Tx. At the receiver, the channel impulse responses (CIRs) were obtained by slide-correlating the received signals with a synchronized copy of the sequence. Samples that were stored and measured from the Rx of the sounder have the baseband in-phase and quadrature-phase (I/Q) signal data format as one datum

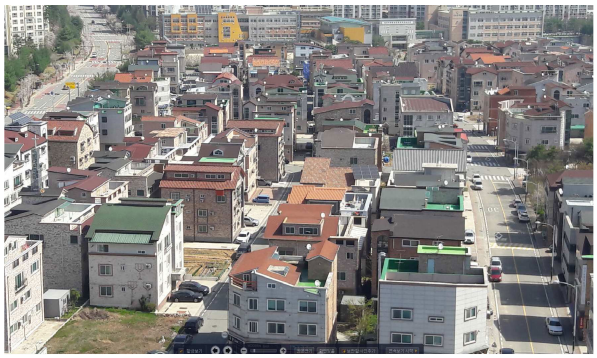

FIGURE 2. A small town (suburban) environment in Korea [17].

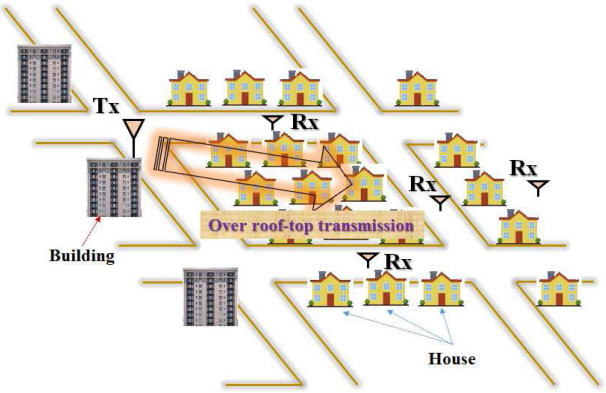

FIGURE 3. Environment for the over-rooftop transmission.

per second. The Tx and Rx were capable of recording the measurement position via a built-in global positioning system (GPS). Directional horn antennas equipped with the Tx or Rx had the same half-power-beam-width (HPBW) of the typical 15 degrees and a directional gain of 21 dBi. The directional horn antenna of the Tx and Rx had an antenna height of 2 meters on the roof of the tall building and 1.5 meters on the ground level, respectively.

B. ENVIRONMENT AND MEASUREMENT

Millimeter wave mobile communication is limited in long distance communication due to its short wavelength. Despite this shortcoming in communication coverage, there is an advantage in that a large amount of data can be transmitted with a wide bandwidth. In millimeter-wave communication, it is very important to establish a communication environment and maintain communication links because transmission loss is high and communication efficiency is less than that of relatively low frequency bands.

Considering these characteristics, we carefully selected a measurement site for suburban environments consisting of three- or four-story houses up to about five hundred meters apart and including adjacent roads, parks, and trees. Each house had a glass window arranged in a reinforced concrete building as shown in Figure 2. As shown in Figure 3, in order to predict the characteristics of transmission loss, the Tx was installed at the top of the roof of the tallest commercial building in the area to be studied, and the small town was selected to exemplify suburban environments in Korea. In this small town in Korea, houses were spaced apart, and the height of most houses was nine to twelve meters above ground level; rooftops were either flat or inclined. Roads had two lanes with sidewalks and streetlamps on both sides. There was a park in the town, surrounded by conifer trees. Overall, the houses were built on well-maintained roads. There were also empty lots with no houses. Vehicles parked on roads or parking spaces in front of houses. The propagation characteristics of radio waves on the slant-path above the roofs of houses affected the multipath propagation of radio waves depending on the height of the house, the distance between houses, and the placement of the surrounding roads.

Figure 3 shows the environments of propagation for over-rooftop paths above the houses built on well-maintained roads. The Tx was installed on the tallest building. The Rx was located between houses. The antenna height of the Rx was relatively lower than the height of the average house.

Figure 4 shows the radio propagation characteristics for the over-rooftop pathway; refer also to Table 1 for the measurement system and environment information. The antenna height (h_{Tx}) of the Tx installed on the roof of the building was 44 meters above the ground level, and the antenna height (hRx) of the mobile Rx located below the houses was 1.5 meters above the ground level. The Tx antenna was the directional horn antenna with an HPBW of the typical 15 degrees. The beam-width of the transmitting antenna covered all the area to be studied. The Rx antenna had a directional beam pattern. When measuring the real environment, the Tx antenna was tilted down to face the edge of the roof and pointed toward the house in front of the Rx. The down-tilted angles from 4 to 37 degrees were adjusted according to the distance of the transceiver and the height of the roof of the front house. The closer the Tx was, the larger the tilt elevation. The modulated radio signal emitted from the Tx hit the rooftop edge of the house in front of the Rx; it was diffracted and propagated through the walls of the back house and the walls of the front house to the height of the Rx by reflection off the wall. However, there could be a path that reached the height of the Rx while reflecting back to the wall of the front house by reflection off the wall of the back house. If there was no house behind the Rx, it could be inferred that the signal was directly transmitted to the Rx through diffraction off the roof's edge of the front house.

The above characterized a transmission characteristic for the NLoS region. For the LoS region, various paths were considered, such as a signal reflected through direct waves, a signal received through the outer wall edge of the house, and a signal received against the wall of the back house. In this study, the basic transmission loss was derived from the statistical results of the signals received at the Rx measurement locations in the site-general environment without distinguishing these various propagation path char-

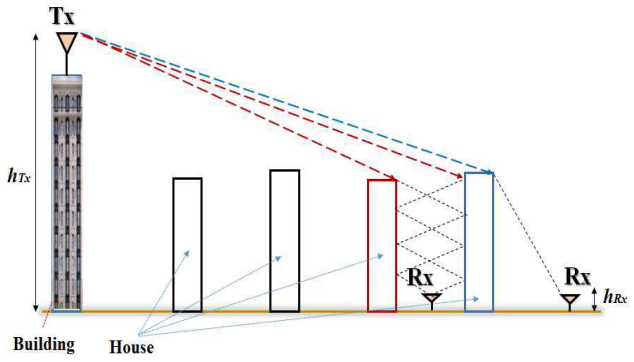

FIGURE 4. Radio characteristics for the over-rooftop transmission.

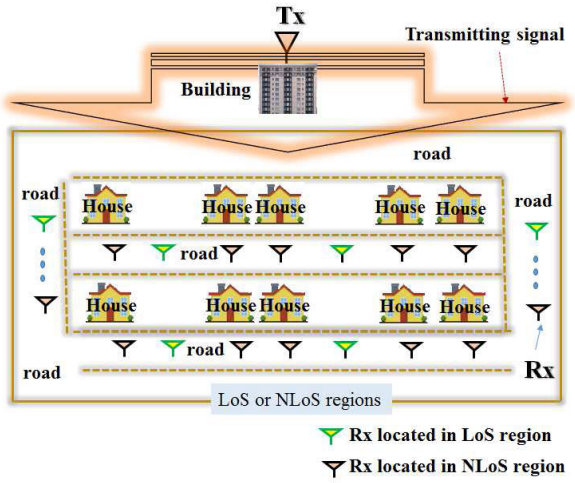

FIGURE 5. Deployment of the house, road, and movement of the Rx for measuring the signals.

acteristics. Only measurements with signal levels received 10 dB higher than the signal-to-noise ratio of the Rx were considered. The basic transmission loss was inferred using only the measurement data.

Figure 5 shows the Rx moving around the road and around the building to measure the receiving signal level in the small town. If the Rx was no longer visible to the Tx above the building while the Rx was moving, this point is depicted as an NLoS point (brown antenna symbol). If the Rx was visible, this point is depicted as a LoS point (green antenna symbol). In this paper, basic transmission loss is derived by dividing LoS and NLoS regions for the small town. In the next section, to find the basic transmission loss, data for LoS and NLoS at each measurement point will be classified and used to derive the overall basic transmission loss model according to location variation.

In Figure 2, measurements were made for the suburban environment in Korea. Figures 6 and 7 show overhead satellite images, where the yellow dotted line indicates the measurement area, divided into visible (LoS region) and invisible (NLoS region) areas, respectively. The LoS region was set to a measuring area of about 400 meters beginning

FIGURE 6. LoS measurement in unit area (150m × 350m).

60 meters away from the Tx point, and the unit area of the visible area was from 150 to 350 meters.

The invisible area was set to the measurement area of about 500 meters beginning 250 meters away from the Tx point, and the unit area of the invisible area was from 200 to 250 meters. The measurement ranges for the visible and invisible areas were divided according to the layout of the houses and roads. When looking at the measurement areas from the transmission point located on the high building for the over-rooftop path, there could be visible areas where the road was constructed parallel to the antenna direction. On the other hand, if the road was perpendicular to the antenna direction, there were many points behind the building where the receivers were not visible. As shown in Figures 6 and 7, the road was vertical in the area close to 250 meters from the transmitting point. After that, it can be seen that the road was constructed in the horizontal direction.

III. LOCATION VARIABILITY BASED ON MEASUREMENT

A. APPROACH ON ANALYTICAL METHODOLOGY

For location variability analysis based on measurement data, measurement was conducted from 63 to 514 meters. Figures 6 and 7 show the unit area of the LoS and NLoS regions.

Location percentage was statistically representative of change over a given unit area in signal strength of the radio propagation channel due to changes in terrestrial environment and is defined as probability with which a given statistically varying signal strength exceeds a specific percentage value, taking into account the location variability (i.e. the statistical fluctuation relates to the variability of the signal strength over a given unit area) of all signals involved [18]. The change in signal strength was obtained for a given unit area, which was defined as "150m × 350m" in the LoS and "200m × 250m" in the NLoS region. A method of

FIGURE 7. NLoS measurement in unit area (200m × 250m).

parameter derivation, considering the percentage of the location, was mentioned in the Recommendation ITU-R P.1411 [7]. This source provides an analytical methodology for below-rooftop paths rather than over-rooftop paths in outdoor environments. However, it is useful for deriving the basic transmission loss model for over-rooftop paths in sub-urban environments. The procedure for statistically modeling changes in locational characteristics is as follows: First, the data obtained from the measured fields were divided into the LoS and NLoS areas to derive their respective basic transmission loss values. Then, based on the suitability of the measured signal values, the difference between measurement data and median curve-fitting line according to Rx to Tx distance in Figure 8 was calculated. To express the statistics of location variability in our empirical basic transmission loss model, the best-fit distribution was extracted from the CDF of the residuals. Location correction factor reflecting location variability as the function of location percentage was derived from the inverse-CDF of the best-fit distribution. Finally, our empirical basic transmission loss model over a given unit area in LoS and NLoS regions established a statistical model from adding the location correction factor based on the location percentage by the median curve-fitting line.

B. BASIC TRANSMISSION LOSS

The given distance from a transmission point indicates the maximum radius, not the distance traveled. The actual number of measurement points in each region were 45 points in the LoS region and 124 points in the NLoS region. The expected radius of future millimeter wave communications is about 500 meters in outdoor environments. Figure 8 shows the basic transmission loss according to the given distance (Rx to Tx distance is plotted on a log scale) along the receiving point from the transmission point. The basic

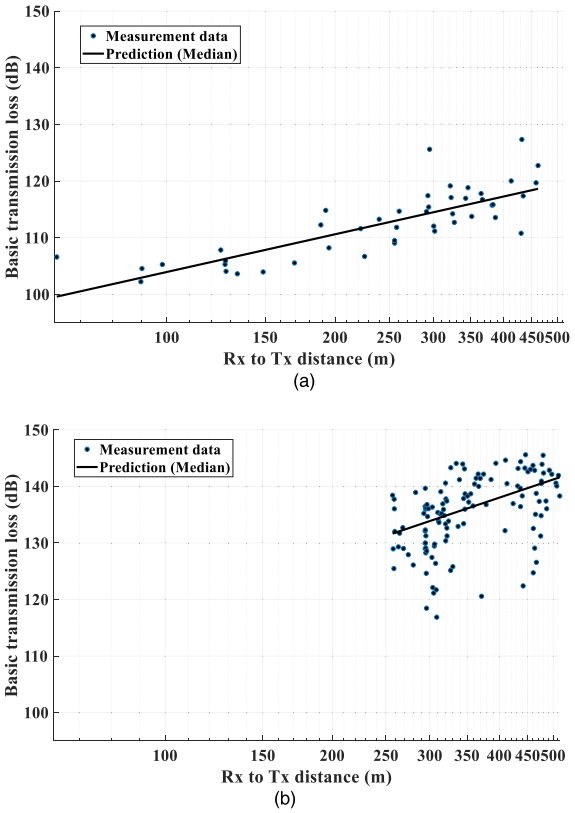

FIGURE 8. Measured basic transmission loss values plotted against Rx to Tx distance on a log scale: (a) LoS and (b) NLoS.

transmission loss was derived based on the measured data. As the given distance increased, the value of the basic transmission loss was greatly dispersed due to the change in position. The distribution of the long-range LoS signals can be seen in Figure 8(a) and the short-range NLoS signals in Figure 8(b). In general, the distance-dependent basic transmission loss value appeared to follow the normal basic transmission loss model, considering the standard deviation of the received signal strength over the given distance. The basic transmission loss had a path loss characteristic according to the transmission and reception distances for a specific operating frequency and a long-term (shadow) fading characteristic, according to a reception degree of a multipath signal at each given distance. Therefore, it was necessary to consider what factors affected the main parameters that represent basic transmission loss and to derive the effect in real environments. Here, the main parameters can be considered frequency, distance, and environmental factors, such as dense urban or urban high-rises or suburban.

In this paper, basic transmission loss was derived based on the operating frequency of 32.4 GHz, given distance from 63 meters up to 514 meters, in a suburban environment with three- or four-story buildings. The basic transmission loss ("*BTL*") is expressed by equation (1), and each parameter is defined as follows.

$$\mathrm{BTL}(d) = 10 \cdot \alpha \cdot \log_{10}(d) + \beta + N(0, \sigma^2) \qquad (1)$$

where

d:	Rx to Tx distance (m)
α:	the coefficient associated with the increase of basic transmission loss with the distance
β:	the coefficient associated with the offset value of basic transmission loss with frequency
$N\ (0, \sigma^2)$:	zero mean Gaussian random variable with a standard deviation, σ (dB)

However, the exponent of the coefficient for each parameter should be derived from the actual environmental measurements. Different LoS and NLoS environments have different coefficients associated with a median basic transmission loss. The median basic transmission loss factor over distance for over-rooftop paths is larger than the median free space loss ("TL_{FS}") in equation (2) for LoS ("TL_{LoS}") as well as for NLoS ("TL_{NLoS}"). The following equations (3–4) as the median basic transmission loss models based on measurement data show the curve-fitting results according to the environment shown in Figure 8 for over-rooftop paths in suburban environments. In equation (2), λ depicts the wavelength.

$$\mathrm{TL}_{FS}(d) = 20.0 \cdot \log_{10}(4\pi d/\lambda) \quad \text{in free space} \tag{2}$$

$$\mathrm{TL}_{LoS}(d) = 22.1 \cdot \log_{10}(d) + 60.0 \quad \text{in LoS} \tag{3}$$

$$\mathrm{TL}_{NLoS}(d) = 33.1 \cdot \log_{10}(d) + 51.0 \quad \text{in NLoS} \tag{4}$$

As the results shown in Figure 8 and derived from equations (3–4) indicate, the power attenuation was 2.21 according to the distance in the LoS region at the 32.4 GHz band for the over-rooftop in the small town. The power attenuation was 3.31 according to the distance in the NLoS invisible region. In the site-general characteristics for a small town (suburban) environment, the standard deviation (σ) values of the LoS and NLoS environments were 3.47 dB and 5.70 dB, respectively.

C. STATISTICAL PROBABILITY DISTRIBUTION OF LOCATION VARIATION

As shown in Figure 8, the basic transmission losses over a given unit area will vary depending on the surrounding environment even at the same Rx to Tx distance. To express the statistics of this location variability over a given unit area, the best-fit distributions for LoS and NLoS regions were extracted from the cumulative probability of the residual values as shown in Figure 9. The residual values mean the difference values between the measurement data given in Figure 8 and values of median curve-fitting line according to Rx to Tx distance given by equations (3–4) in LoS and NLoS regions, respectively. Figure 9 shows the CDF of the residuals based on measurement data and shows the CDFs of approximate prediction distributions. The variation of path attenuation values in the LoS and NLoS regions for over-rooftop path propagation could be slightly different with the general Gaussian random distribution ("Normal"). To derive the optimal prediction model for location variability according to the urban or suburban environment, it was

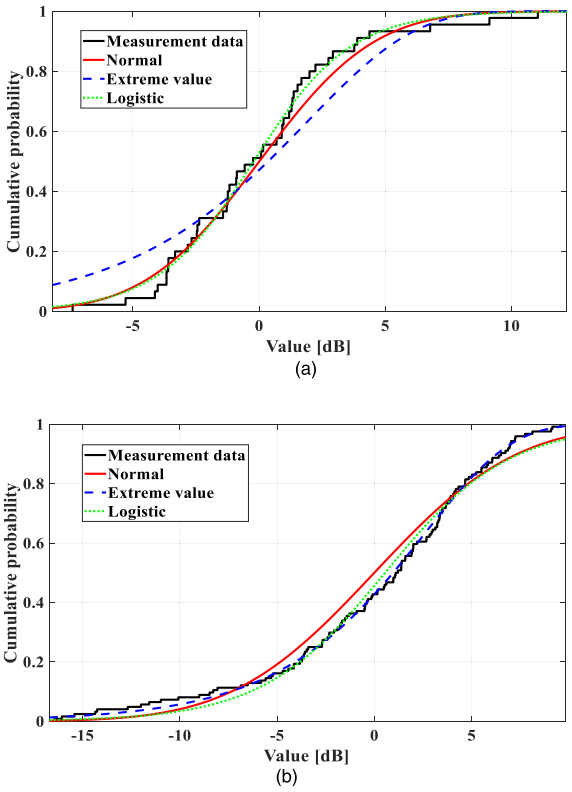

FIGURE 9. Cumulative distribution functions of location variability: (a) LoS and (b) NLoS.

necessary to find out the best-fit distribution for the LoS and NLoS regions. It was possible to apply statistical analysis to obtain CDFs, as shown in Figure 9, by investigating the deviation between the measurement data ("Measurement") and median fits ("Normal," "Extreme value," "Logistic"). As shown in Figure 9, Logistic and Extreme value distributions were best represented, respectively, by the LoS and NLoS regions. This is similar to the tendency of the signal distribution variations in the measurement environment. Values shown in Figure 9 provide an idea of the change in signal strength received during the measurement process in LoS and NLoS environments. Location correction factor as the statistical function of location percentage was clearly defined as the inverse-CDF of the statistical distribution in Recommendation ITU-R P.1411 [7] and P.1546 [18]. In our paper, the location correction factors reflecting location fluctuation based on measurement data were quantified from the inverse-CDF of the best-fit distributions of residuals in LoS and NLoS regions, respectively. As a result of the reviewed CDFs, it was reasonable to consider LoS and NLoS models of location variability in Logistic and Extreme value distributions. LoS regions showed slight deviations in a small number of data items compared to the NLoS regions. Sometimes, the proximity of the transmitter could significantly improve values due to beam width and antenna pattern issues.

More specifically, the following equations (5–6) show that the location correction added to the median value of the basic

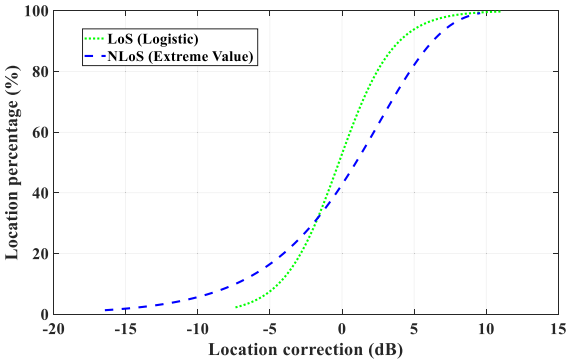

FIGURE 10. Location correction (ΔL) corresponding to the percentage of location.

transmission losses in LoS and NLoS regions was a function of location percentage ("p") given by

$$\Delta L_{Logistic}(p) = Logistic^{-1}(p/100) \quad \text{in LoS} \tag{5}$$
$$\Delta L_{Extreme}(p) = Extreme^{-1}(p/100) \quad \text{in NLoS} \tag{6}$$

where, $Extreme^{-1}(\cdot)$ and $Logistic^{-1}(\cdot)$ represent the inverse-extreme-value CDF and the inverse-logistic CDF, respectively [19].

The location correction curves for each location percentage by equations (5-6) are shown in Figure 10 and are represented by the best-fit distributions of location variability in Figure 9. The slope of the CDF curve of the location correction of the residuals represents the effect of location percentage. If the curve were perfectly vertical, the location corrections would all be the same. In this case, the location correction was null. The longer the slope, the greater the impact due to the location change.

IV. PROPOSED MODEL BASED ON LOCATION VARIABILITY

A. PROPOSED EMPIRICAL MODEL

The proposed empirical basic transmission loss ("LTL_{LoS}", "LTL_{NLoS}") in dB at distance d in meters adds the location correction ("$\Delta L_{Logistic}$", "$\Delta L_{Extreme}$") in equations (5–6) by the median ("TL_{LoS}", "TL_{NLoS}") of LoS or NLoS losses in equations (3–4), given by equations (7–8)

$$\mathrm{LTL}_{LoS}(d,p) = TL_{LoS}(d) + \Delta L_{Logistic}(p) \quad \text{in LoS} \tag{7}$$
$$\mathrm{LTL}_{NLoS}(d,p) = TL_{NLoS}(d) + \Delta L_{Extreme}(p) \quad \text{in NLoS} \tag{8}$$

The location corrections for $p = 1$, 10, 50, 90, and 99% are given in Table 2. This model has not been tested for $p < 1\%$. The statistics were obtained from the study area.

Figure 11 shows the empirical basic transmission losses obtained by applying the location percentage based on the measurement data. Due to the approximate logistic or extreme value variation of the signal, it is possible to calculate the values of the signal strength which is exceeded at a specific percentage, p, of the locations for terrestrial paths within a given unit area. The black circles represent the measured

TABLE 2. LoS and NLoS location variability corrections.

p (%)	$\Delta L_{Logistic}$ (dB)	$\Delta L_{Extreme}$ (dB)
1	9.0	17.8
10	4.4	7.4
50	0.2	1.0
90	-4.0	-6.3
99	-8.6	-9.4

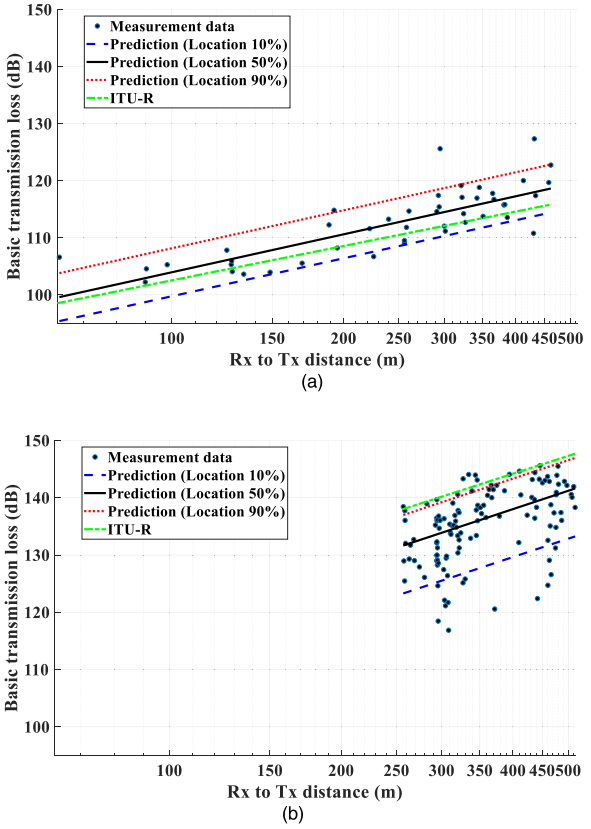

FIGURE 11. Curve of the basic transmission loss not exceeded for 10 %, 50 %, and 90 % of locations plotted against Rx to Tx distance on a log scale in (a) LoS and (b) NLoS.

data ("Measurement data"), and the blue dashed line, black solid line, and red dotted line represent the results obtained by applying location percentages of 10 % ("Prediction (Location 10%)"), 50 % ("Prediction (Location 50%)"), and 90 % ("Prediction (Location 90%)"), respectively. We also calculated the site-specific basic transmission loss (ITU-R) of the over-rooftop path for suburban areas provided by the Recommendation ITU-R P.1411 [7], showing the results through the green dash-dotted line in Figure 11 (Calculation conditions: station 1 antenna height, $h_1 = 44$ m, station 2 antenna height, $h_2 = 1.5$ m, average height of buildings, $h_r = 10$ m, street width, $w = 15$ m, street orientation with respect to the direct path, $\varphi = 90°$). The difference between the median curve for measurement basis and the ITU-R prediction curve was due to the propagation environment of

the electromagnetic wave [17], [20], [21]. The ITU-R curve appears to show the approximate results of the site-specific prediction model where the buildings were the same height and there were no gaps between buildings, while the median curve based on the measurement data shows the analyzed results in a real environment, as shown in Figure 2, where the characteristics of the roofs of buildings varied in from flat to sloped and there were gaps between buildings. Thus, various multipath characteristics received between buildings were additionally reflected to cause the difference. The reason why LoS was larger than the free space loss was because it was additionally affected by multipath reflection. In the case of NLoS, compared to the ITU-R model, multipath signals, such as reflected signals flowing between buildings and diffraction in the real environment, were merged, which caused the relative path loss characteristics to be reduced.

If the location percentage, p, is given as an independent variable of the inverse-CDF, the basic transmission loss is determined as the dependent variable accordingly. This dependent variable refers to the location correction. Therefore, we can understand that the corrected basic transmission loss value is the worst value among randomly generated values by the definition of the inverse cumulative distribution function. In more detail, if a certain location percentage is determined, the basic transmission loss value is corrected by the previous procedure to draw a new regression curve, and it can be interpreted that the corrected regression curve means the worst line that can generate the basic transmission loss value.

It is expected that this statistical model can be used as an indicator for communication designers to choose between cost and performance. The proposed empirical basic transmission loss can show differences due to spatial changes, such as distance and house density in suburban as well as the planned urban environment. Therefore, it is necessary to statistically model changes in the radio wave propagation characteristics due to changes in the surrounding environments.

V. CONCLUSIONS

This paper measured the change in propagation characteristics according to the location variability of suburban environments at 32 GHz bands. A statistical distribution was provided to characterize the received signal position behavior, and a set of threshold parameter values for this distribution was calculated from the measurement data. In location percentage analysis, logistic and extreme value distributions were first found to be suitable for LoS and NLoS location points. Location variations depended on the density of the houses and roads based on the location at which the operation of the received signal was measured for the over-rooftop path in a suburban environment, which could lead to a high standard deviation. Future work concerns differences due to spatial changes such as house density for the over-rooftop paths in the planned urban environment.

REFERENCES

[1] M. R. Akdeniz, Y. Liu, M. K. Samimi, S. Sun, S. Rangan, T. S. Rappaport, and E. Erkip, "Millimeter wave channel modeling and cellular capacity evaluation," *IEEE J. Sel. Areas Commun.*, vol. 32, no. 6, pp. 1164–1179, Jun. 2014.
[2] G. R. MacCartney, J. Zhang, S. Nie, and T. S. Rappaport, "Path loss models for 5G millimeter wave propagation channels in urban microcells," in *Proc. IEEE Global Commun. Conf. (GLOBECOM)*, Dec. 2013, pp. 3948–3953.
[3] T. S. Rappaport, *Wireless Communications, Principles and Practice*. Upper Saddle River, NJ, USA: Prentice-Hall, 1996.
[4] J. Lee, M.-D. Kim, J.-J. Park, and Y. J. Chong, "Field-measurement-based received power analysis for directional beamforming millimeter-wave systems: Effects of beamwidth and beam misalignment," *ETRI J.*, vol. 40, no. 1, pp. 26–38, Feb. 2018.
[5] D. He, B. Ai, K. Guan, Z. Zhong, B. Hui, J. Kim, H. Chung, and I. Kim, "Stochastic channel modeling for railway tunnel scenarios at 25 GHz," *ETRI J.*, vol. 40, no. 1, pp. 39–50, Feb. 2018.
[6] S. A. Busari, S. Mumtaz, S. Al-Rubaye, and J. Rodriguez, "5G millimeter-wave mobile broadband: Performance and challenges," *IEEE Commun. Mag.*, vol. 56, no. 6, pp. 137–143, Jun. 2018.
[7] *Propagation Data and Prediction Methods for the Planning of Short-Range Outdoor Radiocommunication Systems and Radio Local Area Networks in the Frequency Range 300 MHz to 100 GHz*, Standard ITU-R P.1411-10, ITU, Geneva, Switzerland, Jun. 2019.
[8] *European Cooperation in the Field of Scientific and Technical Research EURO-COST231, Urban Transmission Loss Models Mobile Radio in the 900 and 1800 MHz Bands*. The Hague, The Netherlands, 1991.
[9] N. Kita, W. Yamada, and A. Sato, "Path loss prediction model for the over-rooftop propagation environment of microwave band in suburban areas," *Electron. Commun. Jpn.*, vol. 90, no. 1, pp. 13–24, Jan. 2007.
[10] P. Valtr, J. Zeleny, P. Pechac, and M. Grabner, "Clutter loss modelling for low elevation link scenarios," *Int. J. Antennas Propag.*, vol. 2016, pp. 1–4, Apr. 2016.
[11] M. M. Ahamed and S. Faruque, "Propagation factors affecting the performance of 5G millimeter wave radio channel," in *Proc. IEEE Int. Conf. Electro Inf. Technol. (EIT)*, May 2016, pp. 728–733.
[12] J. Lee, J. Liang, M.-D. Kim, J.-J. Park, B. Park, and H. K. Chung, "Measurement-based propagation channel characteristics for millimeter-wave 5G Giga communication systems," *ETRI J.*, vol. 38, no. 6, pp. 1031–1041, Dec. 2016.
[13] A. I. Sulyman, A. T. Nassar, M. K. Samimi, G. R. Maccartney, T. S. Rappaport, and A. Alsanie, "Radio propagation path loss models for 5G cellular networks in the 28 GHZ and 38 GHZ millimeter-wave bands," *IEEE Commun. Mag.*, vol. 52, no. 9, pp. 78–86, Sep. 2014.
[14] I. Rodriguez, H. C. Nguyen, T. B. Sorensen, J. Elling, J. A. Holm, P. Mogensen, and B. Vejlgaard, "Analysis of 38 GHz mmWave propagation characteristics of urban scenario," in *Proc. Eur. Wireless*, May 2015, pp. 374–381.
[15] H. Xu, T. S. Rappaport, R. J. Boyle, and J. H. Schaffner, "Measurements and models for 38-GHz point-to-multipoint radiowave propagation," *IEEE J. Sel. Areas Commun.*, vol. 18, no. 3, pp. 310–321, Mar. 2000.
[16] J. Lee, K. Kim, M. Kim, J. Park, Y. K. Yoon, and Y. J. Chong, "Millimeter-wave directional-antenna beamwidth effects on the ITU-R building entry loss (BEL) propagation model," *ETRI J.*, vol. 42, no. 1, pp. 7–16, Feb. 2020.
[17] Y. K. Yoon, K. W. Kim, and Y. J. Chong, "Site prediction model for the over rooftop path in a suburban environment at millimeter wave," *Int. J. Antennas Propag.*, vol. 2019, pp. 1–12, Apr. 2019.
[18] *Method for Point-to-Area Predictions for Terrestrial Services in the Frequency Range 30 MHz to 4000 MHz*, Standard ITU-R P.1546-6, ITU, Geneva, Switzerland, Aug. 2019.
[19] K. Krishnamoorthy, *Handbook of Statistical Distributions With Applications*. Boca Raton, FL, USA: CRC Press, 2016.
[20] C. Kim and Y. B. Park, "Prediction of electromagnetic wave propagation in space environments based on geometrical optics," *J. Electromagn. Eng. Sci.*, vol. 17, no. 3, pp. 165–167, Jul. 2017.
[21] J. H. Lee, J. Kim, Y. Kim, S. Kim, D.-S. Kim, Y. Lee, and J.-G. Yook, "Attenuation effects of plasma on ka-band wave propagation in various gas and pressure environments," *J. Electromagn. Eng. Sci.*, vol. 18, no. 1, pp. 63–69, Jan. 2018.

YOUNGKEUN YOON received the B.S. degree in electrical engineering and the M.S. and Ph.D. degrees in radio communication engineering from Chungbuk National University, Cheongju, South Korea, in 1991, 1999, and 2007, respectively. Since 2000, he has been working with the Electronics and Telecommunications Research Institute, Daejeon, South Korea, where he is currently a Senior Member. His main research interests are in radio propagation, communication, and artificial intelligence-based on radio communication.

SANGWOOK PARK received the B.S. and M.E. degrees in radio science and engineering from Chungnam National University, Daejeon, South Korea, in 2003 and 2005, respectively, and the Ph.D. degree from the University of Electro-Communications (UEC), Tokyo, Japan, in 2008.

In 2008, he joined UEC, where he was an Assistant Professor with the Department of Information and Communication Engineering. From 2009 to 2013, he was a Researcher with the National Institute of Information and Communications Technology, Tokyo. From 2013 to 2018, he was a Senior Researcher with the Korea Automotive Technology Institute, Cheonan, South Korea. Since 2019, he has been an Assistant Professor with the Division of Electronic and Electrical Engineering, College of Information and Communication Engineering, Daegu University, Gyeongsan, South Korea. His current research interests include electromagnetic interference/electromagnetic compatibility (EMC), microwave transmission circuits, numerical analysis, biomedical EMC, electromagnetic wave propagation, and automotive information and communications technology convergence.

Dr. Park is a member of the Institute of Electronics, Information and Communication Engineers, the Korea Institute of Electromagnetic Engineering and Science, and the Bioelectromagnetics Society. He was a recipient of the Student Award at the 2004 International Symposium on EMC.

JONG HO KIM received the B.S. degree in electrical engineering and the M.S. and Ph.D. degrees in radio communication engineering from Chungnam National University, Daejeon, South Korea, in 1986, 1988, and 2006, respectively. Since 1989, he has been working with the Electronics and Telecommunications Research Institute, Daejeon, where he is currently a Senior Member. His main research interests are in radio wave propagation, mobile communication, and antennas.